Perturbation Formulas for Microstrip Patch Arrays and Elements

Marat Davidovitz, *Senior Member, IEEE*

***Abstract*—One-term perturbation formulas are derived to characterize periodic microstrip arrays with nonuniform planar distributions of dielectric and magnetic materials. Analogous results are also obtained for single-patch elements. The formulas are generally applicable to other types of antennas.**

***Index Terms*—Antennas, microstrip arrays, perturbation methods.**

I. Introduction

An increasing number of phased-array designs utilize microstrip patch elements on finite dielectric supports in contrast with the more conventional configurations in which the entire patch array is fabricated on a single uniform slab. The nonuniform planar architecture affords more flexibility in mechanical design and can alleviate surface-wave-related scan-blindness effects [1]. In attempting to design arrays of such elements the engineer is constrained due to a lack of well-established alternatives to using either relatively efficient simulation tools that permit only uniform substrates (the so-called 2.5-D codes) or the more general but computationally more intensive finite-element packages. In many practically useful cases, the gap between the two methods of analysis can be bridged with simple perturbation methods. Specifically, substrate nonuniformities can be viewed as perturbations of the original laterally uniform layers. Provided the perturbations are sufficiently small, such characteristics of the modified configurations as the input impedance can be obtained from the uniform-substrate solutions by means of relatively simple and easily implementable formulas. Derivation of such formulas for periodic arrangements of, as well as single-element, microstrip patches is the primary purpose of this work.

Perturbation formulas to approximate eigenfrequencies of cavities and waveguides with deformed boundaries or small material inclusions, or to calculate reflection coefficients of small scatterers in waveguides are well established, most notably in [2]–[5]. The ideas developed in the cited references are modified here to encompass configurations of interest. Applications to specific practically significant examples are considered.

In Section II, structures with periodic (Floquet) boundary conditions are considered. Transpose operators for this problem are introduced and are subsequently used to write down the relevant "reciprocity" relations and perturbation results. In Section III analogous formulas are stated for finite aperiodic configurations of patch elements. Numerical examples are presented in Section IV.

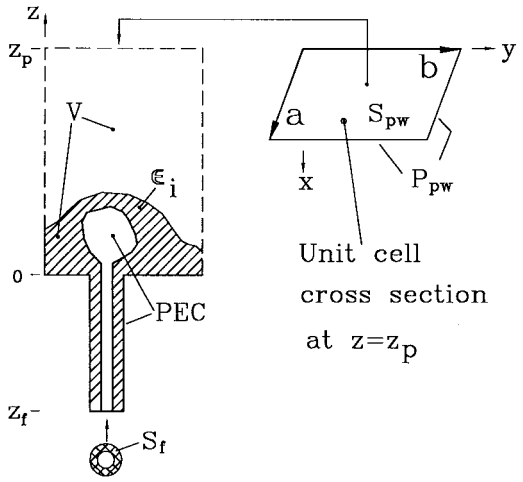

Fig. 1. A unit cell of a periodic antenna array.

II. Periodic Structures

Consider the unit cell of a periodic structure depicted in Fig. 1. Let the periodic lattice be defined by the vector $\mathbf{c}_{mn} = m\mathbf{a}+n\mathbf{b}$, where m, n are integers and the cell vectors $\mathbf{a}, \mathbf{b}$ are shown in the same figure. All subsequent derivations involve two boundary-value problems, namely the unperturbed and the perturbed. The permittivity and permeability distributions will be allowed to differ for these two cases. Descriptions of the two boundary-value problems, distinguished by the subscript $i = 1,2$ follow.[1]

- Maxwell Equations

$$\nabla \times \mathbf{E}_i = -j\omega\boldsymbol{\mu}_i \cdot \mathbf{H}_i \tag{1}$$

$$\nabla \times \mathbf{H}_i = j\omega\boldsymbol{\epsilon}_i \cdot \mathbf{E}_i \tag{2}$$

  where the *material tensors are complex and symmetric*.
- Boundary Conditions: ($\hat{\mathbf{n}} \equiv$ outward unit normal)
  1) Conductors $\hat{\mathbf{n}} \times \mathbf{E}_i = 0$, $\mathbf{r} \in S_{PEC}$.
  2) Floquet Periodicity

$$\left.\begin{aligned}\mathbf{E}_i(\boldsymbol{\rho}+\mathbf{c}_{mn}, z) &= \mathbf{E}_i(\boldsymbol{\rho}, z)\exp[-j\mathbf{k}_{to}\cdot\mathbf{c}_{mn}]\\ \mathbf{H}_i(\boldsymbol{\rho}+\mathbf{c}_{mn}, z) &= \mathbf{H}_i(\boldsymbol{\rho}, z)\exp[-j\mathbf{k}_{to}\cdot\mathbf{c}_{mn}]\end{aligned}\right\} \quad \boldsymbol{\rho}, \mathbf{c}_{mn} \in P_{pw}. \tag{3}$$

Manuscript received May 27, 1997; revised June 16, 1998.

The author is with the Air Force Research Lab/SNHA, Hanscom AFB, MA 01731 USA.

Publisher Item Identifier S 0018-926X(99)04430-0.

[1] A glossary of symbols is available in Appendix A.

3) Input/Output Ports[2]

$$\left.\begin{aligned}\mathbf{E}_{ti} &= \sum_{k=1}^{K} a_{ki} e^{-j\beta_k z_p} \hat{\mathbf{e}}_{pk} \\ \mathbf{H}_{ti} &= \sum_{k=1}^{K} a_{ki} y_{pk} e^{-j\beta_k z_p} \hat{\mathbf{z}} \times \hat{\mathbf{e}}_{pk}\end{aligned}\right\}, \qquad \mathbf{r} \in S_{pw} \tag{4}$$

$$\left.\begin{aligned}\mathbf{E}_{ti} &= \left(e^{-j\beta_{f0} z_f} + R_{0i} e^{j\beta_{f0} z_f}\right) \hat{\mathbf{e}}_{f0} \\ \mathbf{H}_{ti} &= \left(e^{-j\beta_{f0} z_f} - R_{0i} e^{j\beta_{f0} z_f}\right) y_{fo} \hat{\mathbf{z}} \times \hat{\mathbf{e}}_{f0}\end{aligned}\right\} \qquad \mathbf{r} \in S_f \tag{5}$$

where it is assumed that the port surfaces are at sufficient distances along z and of such dimensions that only a single mode on S_f and K propagating modes on S_{pw} have nonzero amplitudes. The subscript "t" denotes transverse-to-z components.

In order to deduce the appropriate perturbation formulas, knowledge is required of the adjoint or transpose operator to that defined in (1)–(5). In the course of the analysis it is found that the operator transpose to (1)–(5) satisfies the same equations with one exception. For the transpose problem the conditions stated (3) differ in the sign of the exponent in the phase term, i.e.,

$$\left.\begin{aligned}\tilde{\mathbf{E}}_i(\boldsymbol{\rho} + \mathbf{c}_{mn},\, z) &= \tilde{\mathbf{E}}_i(\boldsymbol{\rho},\, z)\, \exp[+j\mathbf{k}_{to} \cdot \mathbf{c}_{mn}] \\ \tilde{\mathbf{H}}_i(\boldsymbol{\rho} + \mathbf{c}_{mn},\, z) &= \tilde{\mathbf{H}}_i(\boldsymbol{\rho},\, z)\, \exp[+j\mathbf{k}_{to} \cdot \mathbf{c}_{mn}]\end{aligned}\right\} \quad \boldsymbol{\rho},\, \mathbf{c}_{mn} \in P_{pw} \tag{6}$$

where a "tilde" over a quantity indicates its association with the transpose problem. Physically, under the stated conditions, the transpose problem is identical with the original in every respect except for the 180° change in the scan-angle ϕ_0.

Application of well-known operations [6] to the Maxwell equations (1) and (2) governing the quantities $\mathbf{E}_1$, $\mathbf{H}_1$ and $\tilde{\mathbf{E}}_2$, $\tilde{\mathbf{H}}_2$ leads to the following formula:

$$\begin{aligned}&\nabla \cdot \left(\mathbf{E}_1 \times \tilde{\mathbf{H}}_2 - \tilde{\mathbf{E}}_2 \times \mathbf{H}_1\right) \\ &\quad = -j\omega \left[\mathbf{H}_1 \cdot (\boldsymbol{\mu}_1 - \boldsymbol{\mu}_2) \cdot \tilde{\mathbf{H}}_2 + \mathbf{E}_1 \cdot (\boldsymbol{\epsilon}_2 - \boldsymbol{\epsilon}_1) \cdot \tilde{\mathbf{E}}_2\right].\end{aligned} \tag{7}$$

Before proceeding a choice is made to associate quantities indexed by $i = 2$ with the perturbed problem. Integration of (7) over the domain volume V and application of the divergence theorem yield

$$\begin{aligned}&\iint_{S(V)} \left(\mathbf{E}_1 \times \tilde{\mathbf{H}}_2 - \tilde{\mathbf{E}}_2 \times \mathbf{H}_1\right) \cdot \hat{\mathbf{n}}\, dS \\ &\quad = -j\omega \iiint_V \left[\mathbf{H}_1 \cdot (\boldsymbol{\mu}_1 - \boldsymbol{\mu}_2) \cdot \tilde{\mathbf{H}}_2 + \mathbf{E}_1 \cdot (\boldsymbol{\epsilon}_2 - \boldsymbol{\epsilon}_1) \cdot \tilde{\mathbf{E}}_2\right] dV.\end{aligned} \tag{8}$$

The surface integral can be explicitly evaluated with the aid of the boundary conditions (3)–(5). It is convenient to consider it as a sum of four distinct terms, which are briefly discussed next: 1) the term involving integration over the S_{PEC} portions of the surface $S(V)$ on which the tangential components of *both* $\mathbf{E}_1$, $\tilde{\mathbf{E}}_2$ vanish is identically zero; 2) in view of the radiation condition (4) the integral over S_{pw} does not contribute; 3) although not immediately apparent, the total contribution from the lateral unit cell walls is proven to be zero in Appendix B; and 4) substitution of the field expressions (5) into the surface integral leads to the following result:

$$\iint_{S_f} \left(\mathbf{E}_1 \times \tilde{\mathbf{H}}_2 - \tilde{\mathbf{E}}_2 \times \mathbf{H}_1\right) \cdot \hat{\mathbf{n}}\, dS = 2y_{fo}\left(\tilde{R}_{02} - R_{01}\right). \tag{9}$$

As a result of operations described above, (8) is transformed as follows:[3]

$$\begin{aligned}2y_{fo}(\tilde{R}_{02} - R_{01}) = -j\omega \iiint_V \Big[&\mathbf{H}_1 \cdot (\boldsymbol{\mu}_1 - \boldsymbol{\mu}_2) \cdot \tilde{\mathbf{H}}_2 + \mathbf{E}_1 \\ &\cdot (\boldsymbol{\epsilon}_2 - \boldsymbol{\epsilon}_1) \cdot \tilde{\mathbf{E}}_2\Big] dV.\end{aligned} \tag{10}$$

This expression, combined with appropriate approximations for the fields, is the basis for a one-term perturbation formula for the input reflection coefficient—described briefly in the following paragraphs. However, before proceeding, an interesting consequence of (10) is noted. If the problems corresponding to $i = 1, 2$ are taken to be the same, the right-hand side of (10) vanishes and the following general property of the reflection coefficient is revealed:

$$\tilde{R}_0 = R_0 \tag{11}$$

or in more meaningful notation $R_0(\theta_0,\, \phi_0 + 180°) = R_0(\theta_0,\, \phi_0)$. This fact was proven in [7] using a Fourier expansion of R_0 and the Lorentz reciprocity theorem.

Given the unperturbed solution $\mathbf{E}_1$, $\mathbf{H}_1$, R_{01}, evaluation of the reflection coefficient $\tilde{R}_{02}$ requires knowledge, even if only approximate, of the perturbed fields $\tilde{\mathbf{E}}_2$, $\tilde{\mathbf{H}}_2$. If the perturbation is an electrically small canonical shape, a quasi-static approximation can be derived. Otherwise, the "Born" substitution $\tilde{\mathbf{E}}_2 \approx \tilde{\mathbf{E}}_1$, $\tilde{\mathbf{H}}_2 \approx \tilde{\mathbf{H}}_1$ is made. If valid, the quasi-static approach is typically more accurate.

Substitution of the field approximations into (10) yields the desired perturbation formula. To emphasize the physical interpretation of the results, the notation distinguishing the original and transposed problems by the associated scan direction is adopted in the statement of the final result, which can be written as follows:

$$\begin{aligned}R_{02}(\theta_0,\phi_0) \approx\, &R_{01}(\theta_0,\phi_0) - \frac{j\omega}{2y_{fo}} \iiint_V \mathbf{E}_1(\theta_0,\phi_0 + 180°) \\ &\cdot (\boldsymbol{\epsilon}_2 - \boldsymbol{\epsilon}_1) \cdot \mathbf{E}_{1a}(\theta_0,\, \phi_0) dV \\ &- \frac{j\omega}{2y_{fo}} \iiint_V \mathbf{H}_1(\theta_0,\phi_0 + 180°)(\boldsymbol{\mu}_1 - \boldsymbol{\mu}_2) \cdot \mathbf{H}_{1a}(\theta_0,\phi_0)\, dV\end{aligned} \tag{12}$$

where $\mathbf{E}_{1a}$, $\mathbf{H}_{1a}$ are approximations of the solutions to the perturbed problem, derived in one of the ways already mentioned

[2] It is assumed that the perturbations are finite and do not extend to the port surfaces S_{pw}, S_f.

[3] It is assumed that the feed-line fields are normalized according to the formula stated in Appendix A. This constraint can be removed by changing the normalization constant in the reflection coefficient expressions.

from their unperturbed counterparts $\mathbf{E}_1$, $\mathbf{H}_1$. It is apparent that calculation of the perturbed reflection coefficient R_{02} at a particular scan angle (θ_0, ϕ_0) requires two generally distinct unperturbed solutions at scan angles (θ_0, ϕ_0) and $(\theta_0, \phi_0 + 180°)$. If the structure, symmetries, scan angle, and frequency are such that a waveguide simulator can be constructed, the operator can be made symmetric [7] and the original and transpose solutions will be equal.[4]

III. Finite Antennas

The perturbation formula for nonperiodic structures can be derived along the lines described above. The operators become symmetric. Appropriate radiation conditions replace (3) and (4) in the statement of the problem, e.g., Sommerfeld-type conditions for antennas occupying finite volumes. A more careful treatment is needed for structures having features extending to infinity. In addition to the standard continuous spectrum of plane waves, microstrip antennas on infinite substrates excite surface waves. Specific requirements must be imposed in addition to the standard Sommerfeld condition to ensure that only outgoing surface waves exist at infinity. This issue does not impact the perturbation formulas so long as the perturbed region is finite. Thus, the perturbation formula for the input reflection coefficient can be stated as follows:

$$R_{02} \approx R_{01} - \frac{j\omega}{2y_{fo}} \iiint_V \mathbf{E}_1 \cdot (\boldsymbol{\epsilon}_2 - \boldsymbol{\epsilon}_1) \cdot \mathbf{E}_{1a}\, dV - \frac{j\omega}{2y_{fo}} \iiint_V \mathbf{H}_1 \cdot (\boldsymbol{\mu}_1 - \boldsymbol{\mu}_2) \cdot \mathbf{H}_{1a}\, dV. \quad (13)$$

It should be mentioned that in addition to the input characteristics, the modification of the antenna structure affects the radiation pattern. It is not difficult to write down a formal expression for the perturbed radiation field for a given direction in terms of the unperturbed quantities. However, this would involve the solution of an auxiliary problem in which a plane wave is incident upon the antenna along the same direction. In a more practical approach, the original problem may be solved again with the perturbation terms $\mathbf{J}_p = j\omega(\boldsymbol{\epsilon}_2 - \boldsymbol{\epsilon}_1) \cdot \mathbf{E}_{1a}$, $\mathbf{M}_p = -j\omega(\boldsymbol{\mu}_1 - \boldsymbol{\mu}_2) \cdot \mathbf{H}_{1a}$ treated as sources of the radiation pattern perturbation. Of course, the same approach may be applied to derive formulas equivalent to (12) and (13).

IV. Numerical Examples

Several examples are now offered to illustrate and verify, to the extent possible, the formulas presented in the preceding sections. The solutions of the unperturbed and perturbed problems, as well as the field integrations required to determine the difference between them, were obtained using a commercial, finite-element-based Maxwell equations solver [9]. This approach circumvents the questions of convergence and precision that would have arisen had different methods been used to solve the various problems. Moreover, questions regarding adequacy of operator representation and mesh construction were avoided by using the same mesh for the unperturbed and perturbed configurations, predetermined by adaptive refinement at the highest frequency of interest.

[4] Another important situation occurs when the material tensors are Hermitian. The Hermitian adjoint of the original operator can then be used instead of its transpose.

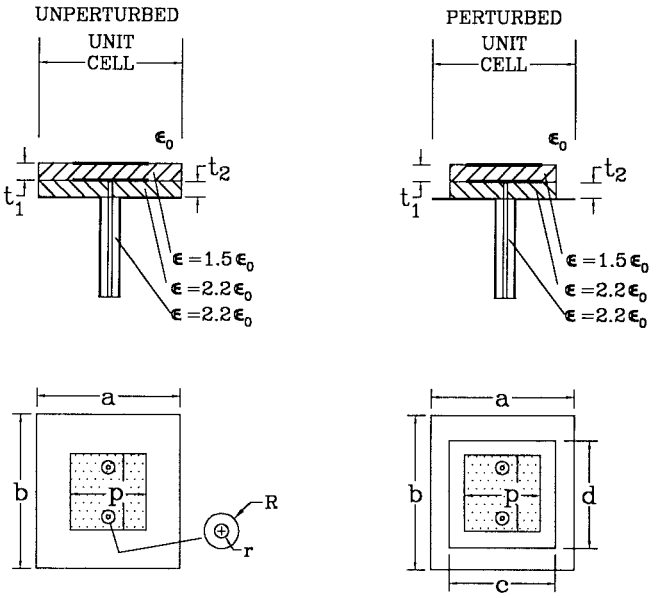

Fig. 2. Unperturbed and perturbed unit cell parameters for an array of two identical square stacked patches with balanced feeds.

An application of (12) to calculate the effect of finite dielectric support for an array of square stacked-patch elements with balanced probe feeds is considered first. Direct verification for all scan angles was not possible because the solver did not allow for Floquet periodicity. Thus, only the portion of the scan-frequency space for which a waveguide simulator can be constructed was accessible. In the unperturbed configuration shown in Fig. 2, the substrate layers uniformly span the entire unit cell. A rectangular outer ring of substrate material is removed in both layers of the perturbed element (Fig. 2), leaving the patches in the periodic array on finite dielectric "islands," separated by free-space. In Fig. 3 input-reflection-coefficient results for an H-plane scan are presented for a specific set of unit cell dimensions and parameters. E-plane scan data are shown in Fig. 4 for the same patch element placed in a somewhat larger unit cell. In both instances (E and H plane) the Born approximation $\tilde{\mathbf{E}}_2 \approx \tilde{\mathbf{E}}_1$ is applied.

Examination of Figs. 3 and 4 leads to several observations:

- The agreement between perturbation-derived and directly computed reflection-coefficient data is quite good in both cases despite the fact that almost 25% and 50%, respectively, of substrate materials is replaced by free-space.
- A likely reason for the quality of the perturbation approach is the fact that the fields are concentrated predominately under the patch elements and are relatively weaker in the interelement spaces. In other words, the measure of the "size" of the perturbation is provided not only by the change in the dielectric constant, but as significantly by the amount of stored energy in the perturbed volume.

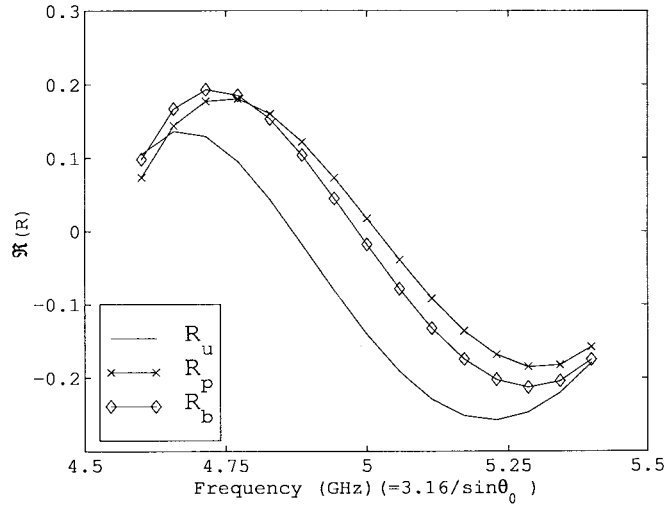

(a)

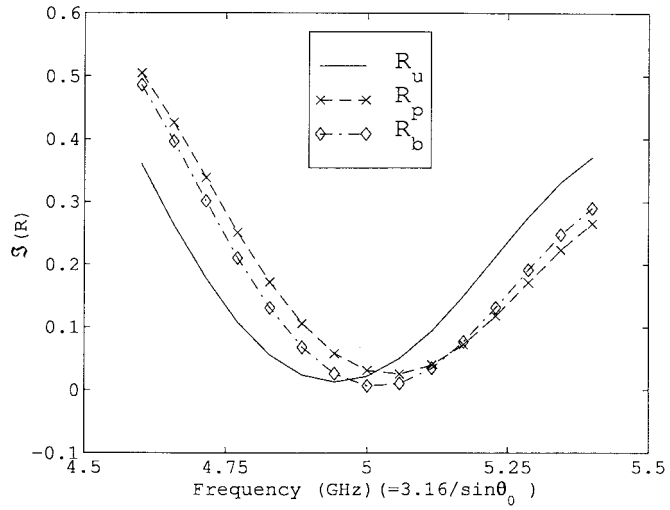

(b)

Fig. 3. H-plane input reflection coefficient: R_u—unperturbed structure; R_p—perturbed structure-direct calculation; R_b—perturbed structure-Born approximation. Unit cell dimensions as defined in Fig. 2 (in centimeters): $a = 2.378$, $b = 2.215$, $c = d = 2.0$, $p = 1.8$, $t_1 = t_2 = 0.159$, $R = 0.155$, $r = 0.045$. (a) Real part ($\Re$) of the reflection coefficient. (b) Imaginary part ($\Im$) of the reflection coefficient. The scan angle θ_0 is measured from broadside.

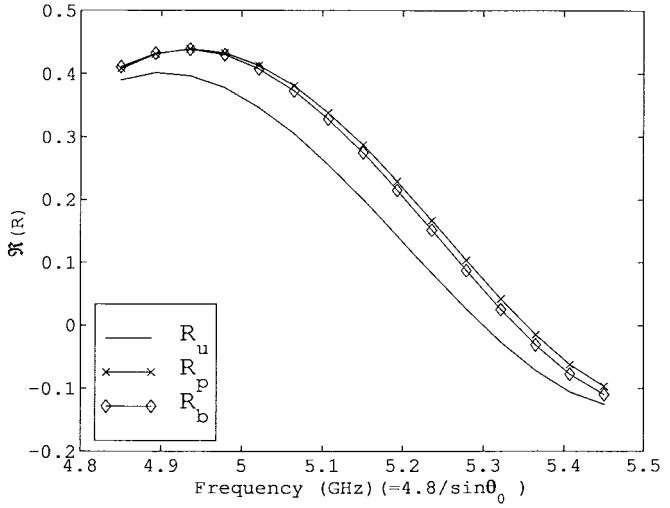

(a)

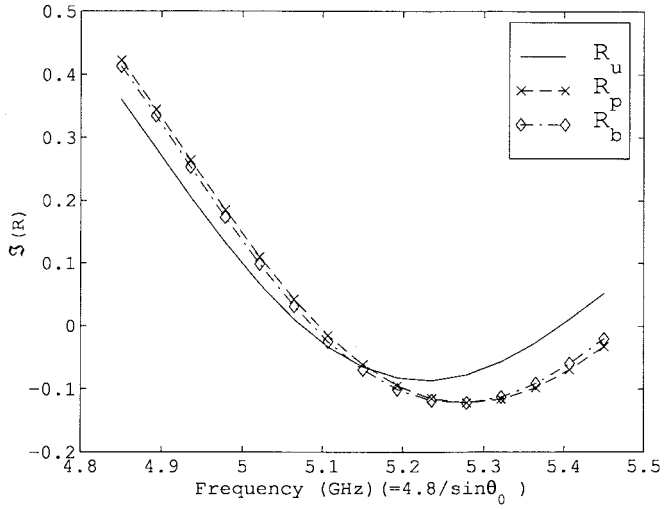

(b)

Fig. 4. E-plane input reflection coefficient: R_u—unperturbed structure; R_p—perturbed structure-direct calculation; R_b—perturbed structure-Born approximation. Unit cell dimensions as defined in Fig. 2 (in cm): $a = 3.0$, $b = 3.125$, $c = d = 2.2$, $p = 1.8$, $t_1 = t_2 = 0.159$, $R = 0.069$, $r = 0.02$. (a) Real part ($\Re$) of the reflection coefficient. (b) Imaginary part ($\Im$) of the reflection coefficient. The scan angle θ_0 is measured from broadside.

Although the derivations were based on coaxially fed radiators, the same formulas can be applied to other transmission line feeds. The simplest way to rationalize the formulas is by conceptualizing lossless perfectly matched transitions from coax to other line types. The example of a single circular patch edge-fed by a microstrip line is used to validate the use of the formulas in more general contexts. The patch in Fig. 5(a) is initially analyzed in free-space. The effect of dielectric support rods is then calculated using the perturbation approach. The comparison of the various data sets is presented in Fig. 5(b) and (c). The dominant electric field component is parallel to the perturbation boundaries and, therefore, the Born and quasi-static approximations coincide. The perturbation formula works well in this situation, even for large values of permittivity.

V. Conclusions

One-term perturbation formulas for the input reflection coefficient were derived for periodic and finite arrangements of antennas. Although intended for microstrip applications, the formulas are general and as such applicable to other antenna types, and can be extended to multiport, open circuit structures. Perturbation formulas for complex resonant frequencies of antennas can also be done. Numerical tests have confirmed that the formulas can be used to predict the effects of substrate perturbations for practical configurations to a good degree of accuracy, despite the use of first-order field approximations. Moreover, the equations can be incorporated into widely used 2.5-D microstrip solvers with only minor additional postprocessing.

Although of great utility, all perturbation approaches of this kind are deficient because it is difficult to gauge the

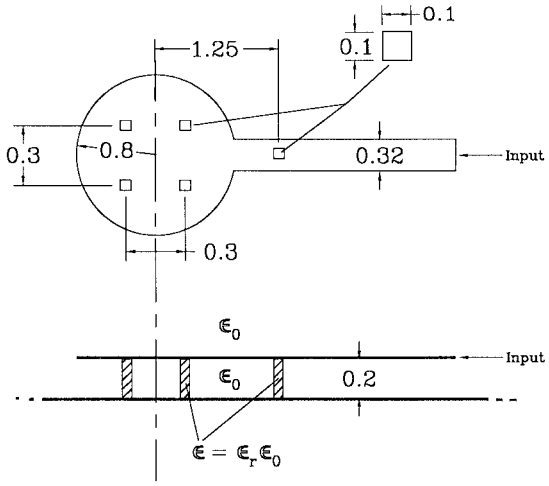

(a)

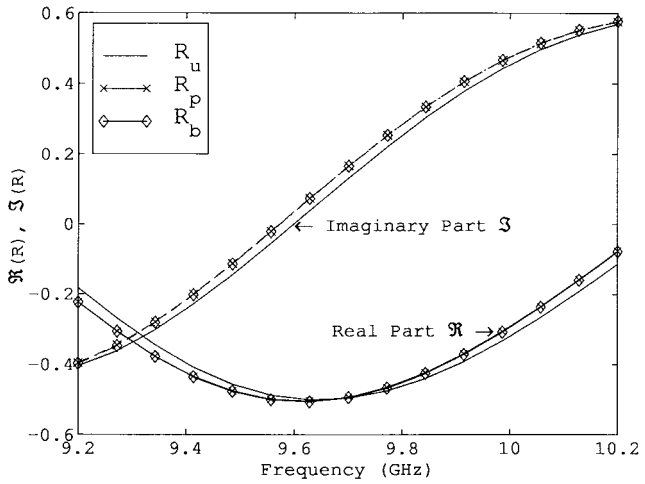

(b)

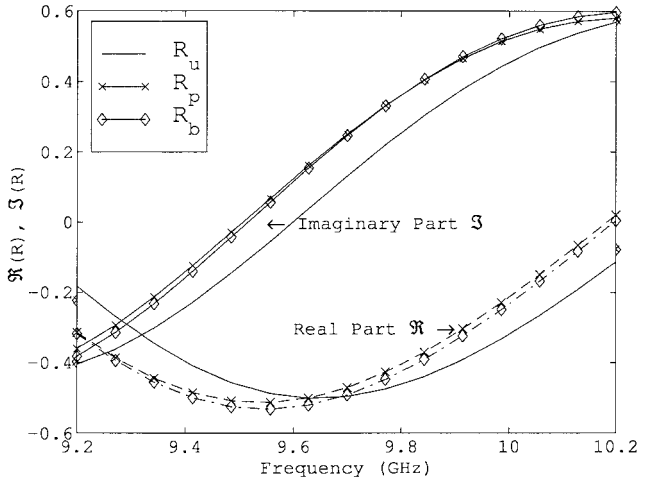

(c)

Fig. 5. (a) Edge-fed circular patch antenna supported by dielectric pins above a ground plane (all dimensions in centimeters). (b) Input reflection coefficient: R_u—unperturbed structure-patch in free-space, R_p—perturbed structure patch on pin supports ($\epsilon_r = 2.2$), R_b—perturbed structure-Born approximation. (c) Input reflection coefficient: R_u—unperturbed structure-patch in free-space, R_p—perturbed structure-patch on pin supports ($\epsilon_r = 5.0$), R_b—perturbed structure-Born approximation.

accuracy of the results. A more self-consistent approach is desirable. Toward that goal, multiterm perturbation expansions are currently under investigation.

Appendix A

(θ_0, ϕ_0)	Scan direction.
$\boldsymbol{\rho} = x\hat{\mathbf{x}} + y\hat{\mathbf{y}}$	
$\mathbf{k}_{to} = k_0(\hat{\mathbf{x}} \sin\theta_0 \cos\phi_0 + \hat{\mathbf{y}} + \hat{\mathbf{y}} \sin\theta_0 \sin\phi_0)$	
$k_0 = 2\pi f/c$	
$P_{pw} = \partial(S_{pw})$	Perimeter of the fundamental unit cell S_{pw}.
$\hat{\mathbf{e}}_{f0}, y_{fo}$	Feed-mode and the associated characteristic admittance; $\int_{S_f} \hat{\mathbf{e}}_{f0} \cdot \hat{\mathbf{e}}_{f0} = 1$.
$\hat{\mathbf{e}}_{pk}, y_{pk}$	Floquet mode and the associated characteristic admittance; $\int_{S_{pw}} \hat{\mathbf{e}}_{pk} \cdot (\widetilde{\hat{\mathbf{e}}_{pk}}) = 1$.
R_{0i}	Input reflection coefficient.

Appendix B

The steps taken to reduce (8)–(10) included integration over the unit cell lateral walls. It is the purpose of this Appendix to show that the said-surface integral vanishes.

The field quantities are subject to the Floquet conditions (3) and as such, may be written as follows:

$$\begin{aligned}\mathbf{E}_i(\boldsymbol{\rho}, z) &= \mathbf{E}_i^P(\boldsymbol{\rho}, z) \exp[-j\mathbf{k}_{to} \cdot \boldsymbol{\rho}] \\ \mathbf{H}_i(\boldsymbol{\rho}, z) &= \mathbf{H}_i^P(\boldsymbol{\rho}, z) \exp[-j\mathbf{k}_{to} \cdot \boldsymbol{\rho}]\end{aligned} \tag{14}$$

where the fields marked by superscript P satisfy periodic boundary conditions

$$\mathbf{A}_i^P(\boldsymbol{\rho} + \mathbf{c}_{mn}, z) = \mathbf{A}_i^P(\boldsymbol{\rho}, z),\ \boldsymbol{\rho}, \mathbf{c}_{mn} \in P_{pw}. \tag{15}$$

Let $\mathbf{F} \equiv \mathbf{E}_1 \times \tilde{\mathbf{H}}_2 - \tilde{\mathbf{E}}_2 \times \mathbf{H}_1 = \mathbf{E}_1^P \times \widetilde{\mathbf{H}_2^P} - \widetilde{\mathbf{E}_2^P} \times \mathbf{H}_1^P$, the last expression reflecting (6) and (14). Moreover, in view of (15) $\mathbf{F}$ satisfies periodicity, i.e., $\mathbf{F}(\boldsymbol{\rho} + \mathbf{c}_{mn}, z) = \mathbf{F}(\boldsymbol{\rho}, z)$, $\boldsymbol{\rho}, \mathbf{c}_{mn} \in P_{pw}$. The surface integral over the lateral walls can be written as follows:

$$\begin{aligned}\iint_{P_{pw} \otimes (z_1, z_2)} \mathbf{F} \cdot \hat{\mathbf{n}}\, dS &= \int_{(z_1, z_2)} dz \int_{P_{pw}} dc\, \mathbf{F}_t \cdot \hat{\mathbf{n}} \\ &= \int_{(z_1, z_2)} dz \iint_{S_{pw}} dS \nabla_t \cdot \mathbf{F}_t\end{aligned} \tag{16}$$

where t marks transverse-to-z components and (z_1, z_2) is the interval of integration along the z axis. The last form of the preceding equation is obtained using the divergence theorem. The integral over S_{pw} vanishes; this can be shown with the aid of the scalar periodic Green's theorem outlined in [8]. Periodicity of $\mathbf{F}_t = F_x\hat{\mathbf{x}} + F_y\hat{\mathbf{y}}$ implies that the integral $I_\tau(\boldsymbol{\rho}') = \int\int_{S_{pw}} F_\tau(\boldsymbol{\rho} + \boldsymbol{\rho}')\, dS$, $\tau = x, y$ is independent of $\boldsymbol{\rho}'$, i.e., the integral does not depend on the choice of the unit cell origin. Therefore, differentiation of this integral with respect to the primed coordinates yields zero, and after the derivatives are moved under the integral sign and applied to the unprimed variables, the aforementioned result is verified.

REFERENCES

[1] M. Davidovitz, "Extension of E-plane scanning range in large microstrip arrays by substrate modification," *IEEE Microwave Guided Wave Lett.*, vol. 2, pp. 491–494, Dec. 1992.

[2] A. D. Berk, "Variational principles for electromagnetic resonators and waveguides," *IRE Trans. Antennas Propagat.*, vol. AP-4, pp. 104–111, Apr. 1956.

[3] R. F. Harrington, *Time-Harmonic Electromagnetic Fields.* New York: McGraw-Hill, 1961.

[4] J. Van Bladel, *Electromagnetic Fields.* New York: Hemisphere, 1985.

[5] V. V. Nikol'skii, *Variational Methods for Interior Electrodynamic Problems.* Moscow, Russia: Nauka, 1967.

[6] L. B. Felsen and N. Marcuvitz, *Radiation and Scattering of Waves.* Englewood, NJ: Prentice-Hall, 1973.

[7] N. Amitay, V. Galindo, and C. P. Wu, *Theory and Analysis of Phased Array Antennas.* New York: Wiley, 1972.

[8] N. W. Ashcroft and N. D. Mermin, *Solid State Physics.* Philadelphia, PA: Saunders College, 1976.

[9] High-Frequency Structure Simulator, Hewlett-Packard, Release 4.0.

Marat Davidovitz (S'81–M'87–SM'95) received the B.S. (highest honors) and M.S. degrees in electrical engineering from the University of Illinois, Chicago, in 1981 and 1983, respectively, and the Ph.D. degree in electrical engineering from the University of Illinois, Urbana-Champaign, in 1987.

From 1987 to 1988, he was an Alexander von Humboldt Postdoctoral Fellow at DLR, Oberpfaffenhofen, Germany. Between 1988 and 1993, he taught at the Department of Electrical Engineering, University of Minnesota, Minneapolis. Since 1994, he has been employed as an Electronics Engineer at the Air Force Research Laboratory, Hanscom AFB, MA.